RESEARCH ARTICLE

Computed tomographic (CT) scan study of the anatomy of grasscutter (*Thryonomys swinderianus*, Temminck 1827): Preliminary observations

Aklesso Ataba[1*], Claude Guintard[2], Mazamaesso Tchaou[3]

[1]Department of Animal and Aquatic Health and Production, Institut Supérieur des Métiers de l'Agriculture (ISMA), University of Kara, Kara, Togo
[2]Comparative Anatomy Unit, Ecole Nationale Vétérinaire Agroalimentaire et Alimentation de Nantes-Atlantique, Oniris – Vet Agro Bio Nantes, Nantes, France
[3]Radiology and Medical Imaging, Faculty of Health Sciences (FSS), University of Kara, Kara, Togo

[*]**Corresponding author:**
Dr. Aklesso Ataba

Address:
Université de Kara, BP 404, Kara, Togo
Phone: +228 92 46 92 82
ORCID: 0009-0003-9360-4291
E-mail: edmonataba@gmail.com

Original Submission: 20 July 2025
Revised Submission: 30 August 2025
Accepted: 4 September 2025

How to cite this article: Ataba A, Guintard C, Tchaou M. 2025. Computed tomographic (CT) scan study of the anatomy of grasscutter (Thryonomys swinderianus, Temminck 1827): Preliminary observations. Veterinaria, 74(3), 237-48.

ABSTRACT

The grasscutter (*Thryonomys swinderianus*) is an African rodent whose breeding has developed in part due to growing scientific interest**.** This work is to investigate the internal anatomy of grasscutter (*Thryonomys swinderianus*) using computed tomography (CT scan). Six grasscutters with an average age of 345 ± 45.63 days and varying sexes and weights, underwent general anesthesia with a ketamine, xylazine mixture and were then subjected to CT scan examination. Volumetric acquisitions were obtained and reconstructed using specific filters: "thoracic or pulmonary tissue," "abdominal tissue," and "bone tissue." Within the thoracic cavity, structures such as the trachea, bronchi, lungs, esophagus, heart, and aorta were identified. In the abdominal cavity, the liver was observed extending transversely from left to right. The stomach, which contained mineral content, as well as the spleen, were clearly identified. The kidneys were also visible, with the left kidney located more cranially than the right. The urinary bladder was identifiable depending on its degree of filling. These same organs have previously been described in rabbits, lemurs, and guinea pigs through CT imaging, supporting comparative anatomical analyses. However, the ureters could not be visualized on the current images. This study represents the first CT scan–based anatomical investigation of the grasscutter and offers valuable insights for applied research in health of this species.

Keywords: Anatomy, computed tomography, grasscutter, X-ray

INTRODUCTION

The grasscutter (*Thryonomys swinderianus*) is a large rodent of the family Thryonomyidae, widely distributed in sub-Saharan Africa. It is traditionally hunted and increasingly raised in captivity for its meat, which is highly appreciated in West African countries. In the wild, it inhabits wetland environments, including reed beds, herbaceous zones, and riverbanks (Mensah et al., 2007; Yapi, 2013).

Interest in this species has increased significantly, as reflected by the expansion of captive breeding and the growing body of scientific literature on its biology and management (Ananivi et al., 2025; Yapi, 2013). Several

doi.org/10.51607/22331360.2025.74.3.237

anatomical studies have investigated its reproductive, nervous, and digestive systems, due to their relevance for understanding its behavior, physiology, and nutritional needs (Broalet et al., 2012; Ibe et al., 2023).

Diagnostic imaging techniques, such as radiography, ultrasonography, computed tomography (CT), and magnetic resonance imaging (MRI) offer effective, non-invasive means to study the anatomy of small mammals. Among them, CT is particularly useful for providing high-resolution cross-sectional images and three-dimensional reconstructions of both soft tissues and bony structures (Ajayi et al., 2010).

Radiographic assessments of the grasscutter have described the thoracic limb, cardiac anatomy, and gestational development (Ibe et al., 2024; Mpagike and Makungu, 2023; Mustapha et al., 2019). However, conventional radiography is limited to two-dimensional views and lacks depth of detail (Tarbell et Fischetti, 2020). CT scanning addresses these limitations by producing fine anatomical slices that allow detailed visualization of internal organs and pathological changes. Nevertheless, interpreting CT images requires prior knowledge of the normal cross-sectional anatomy (Boussarie, 2014).

CT-based anatomical references have been developed for several domestic and laboratory species, including rabbits, guinea pigs, ferrets, dogs, and cats (Winn, 2006; Zotti et al., 2009; Hoey et al., 2013; Calandra, 2016; Husté, 2016; Müllhaupt et al., 2017; Buch et al., 2022). However, no comparable data are currently available for the grasscutter. Therefore, the purpose of the present study was to use CT to investigate the normal thoracic and abdominal anatomy structures of the grasscutter. Specifically, it aims to provide detailed images to support veterinary anatomists, radiologists, and clinicians working with this species, as well as to establish a foundation for further anatomical, diagnostic, and comparative research.

MATERIAL AND METHODS

Ethical Approval

This study was approved by the Health Research Bioethics Committee (CBRS) of Togo under Opinion No. 056/2023/CBRS dated November 2, 2023. All animals were handled in accordance with the Guide for the Care and Use of Laboratory Animals of the National Research Council.

Biological Material

Six clinically healthy adult grasscutters, including three males and three females with a mean age of 345 ± 45.63 days, presented in Table 1, were purchased from local breeders in the Maritime region and included in the study. The average body weight was 4.15 ± 0.55 kg for males and 1.54 ± 0.40 kg for females with the sexual dimorphism reported by Mensah et al. (2007), who reported that males weighed approximately 2.5–4.5 kg and females 2–3 kg at one year of age. The animals were acquired at a young age (2 to 5 months) and fed with panicum and commercially available growing rabbit feed until reaching adulthood (≥ 6 months), at which point anatomical structures are fully developed. Drinking water was provided ad libitum.

Table 1 Characteristics of the grasscutters included in the CT scan study

Sex	Mean Body Weight (kg)	Mean Age (days)
Male	4.15 ± 0.55	373.1 ± 42.77
Female	1.54 ± 0.40	336 ± 48.53

CT Scan Period and Technique

The CT examination was performed in February 2024. The technique described by Boussarie (2014) for rabbits was adapted for this study on the grasscutter, also based on the protocols from Calandra (2016), Huber (2016) and Husté (2016). Imaging was performed using a Neuviz ACE scanner (manufactured in 2020, commissioned in 2021) located at the Human Clinic of Kozah Prefecture. Access to the device was granted exclusively outside of clinic hours.

Preparation and General Anesthesia

Prior to scanning, grasscutters were fasted for 2 to 3 hours. After clinical health assessment and weighing, animals were anesthetized by intramuscular injection

Figure 1 Animal positioning on the CT table: (A) Animal on dorsal recumbency; (B) Animals on lateral recumbency

of a ketamine (0.1 ml/kg body weight) and xylazine (0.5 ml/kg body weight) mixture to ensure complete immobilization during the procedure (Boussarie, 2014; Calandra, 2016; Huber, 2016; Husté, 2016).

Animal Positioning

Four grasscutters were positioned in dorsal recumbency, while two were placed in lateral recumbency shown in Figure 1.

Red laser guides were used to ensure accurate positioning. Animals' bodies were centered along multiple axes prior to image acquisition. The scan parameters are presented in Table 2 and include the following: slice thickness 2 mm, increment 2 mm, 100 kVp, 56 mA, and rotation time of 1 second.

Table 2 CT Scan Parameters

Parameter	Value
Scan Field of View	32 cm
Kilovoltage (kV)	100
mAs	49.7
Milliampere (mA)	56
Number of Images	204
Exposure Duration	29.84 seconds
Slice Thickness	2.00 mm
Slice Increment	2.00 mm
Computed Tomography Dose Index Volume (CTDIvol)	0.0 mGy
Dose Length Product (DLP)	364.8 mGy·cm

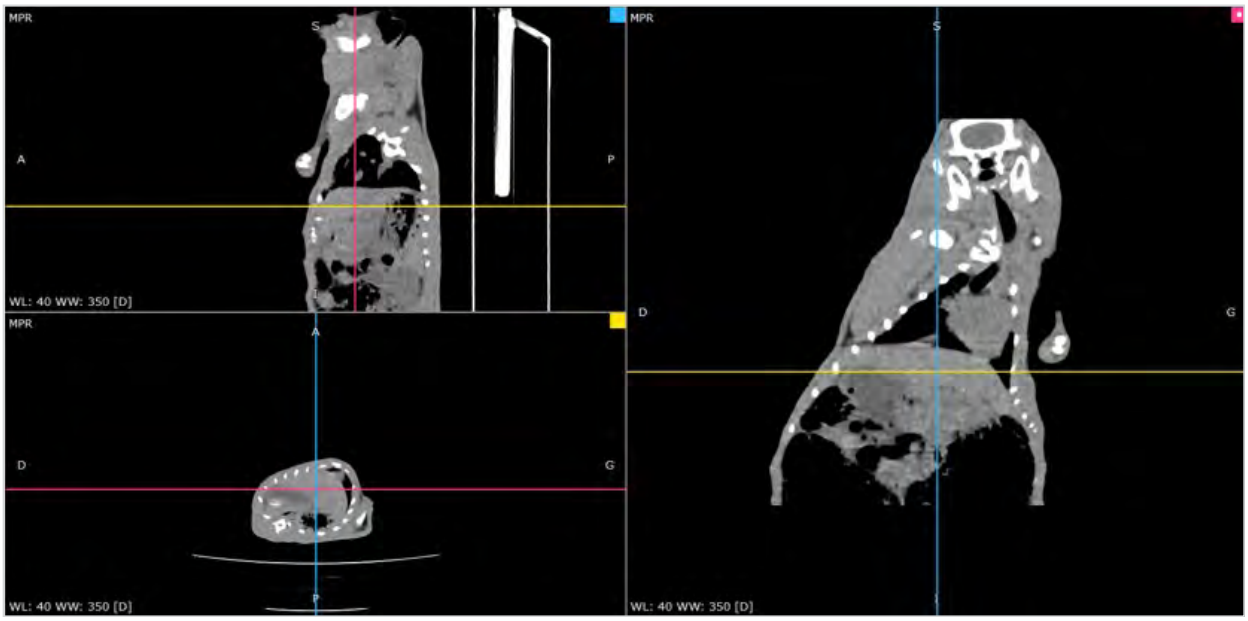

Figure 2 CT image visualization in MPR mode with RADIANT Viewer

Image Processing and Analysis

All volumetric data obtained from the CT examination were visualized using RADIANT Dicom Viewer 2023.1 software, which enabled image reconstruction and identification of anatomical structures. Multiplanar reconstruction (MPR) mode was employed to display transverse, sagittal, dorsal, and coronal planes shown in Figure 2. Additionally, the Minimum Intensity Projection (MinIP) mode facilitated detailed visualization of the respiratory system. Following anatomical recognition, selected transverse and coronal slices were chosen to isolate the greatest number of relevant anatomical structures. Depending on the region, different filters were applied, including « thoracic tissue», « abdominal tissue », « pulmonary tissue », and «bone tissue » filters.

RESULTS

The results of the CT scan examination performed on healthy grasscutters consist of annotated tomographic slice images. The most optimal image quality was obtained when animals were positioned in dorsal recumbency. Tomographic slices obtained using a given reconstruction filter revealed the main anatomical structures, recognizable by their grayscale intensity or anatomical location, and are presented with appropriate legends. On transverse CT sections of the head and neck, the bone filter enabled the identification of osseous structures such as the mandibles, palatine bone, zygomatic arch, and parietal bone (Figure 3).

Between vertebrae C7 and T1, skeletal elements, including the scapula, humerus, radius, ulna, and thoracic and cervical vertebrae, were visualized. Additionally, anatomical passages such as the nasopharynx, tympanic cavity, trachea, and esophagus were clearly delineated. Muscles of the scapular region, notably the infraspinatus and supraspinatus, were also identified on Figure 4.

Using the thoracic soft tissue and pulmonary filters, transverse slices between T7 and T10 allowed clear visualization of the heart, lungs, and main bronchi on Figures 5, 6 and 7. In these sections, the heart occupied a large portion of the mediastinum, while the esophagus and trachea were located dorsally. The two major vessels, the caudal vena cava and the aorta, were also identified.

Observation of the abdominal region with the abdominal soft tissue filter enabled identification of various soft tissue structures. A transverse image at the T10 level revealed the heart, lungs, and liver with distinguishable lobes on both sides. Slices between T10 and T13 shown on Figure 8 allowed identification of the stomach and spleen, with residual mineral contents in the stomach aiding its recognition.

The cecum, clearly visible and voluminous on the left

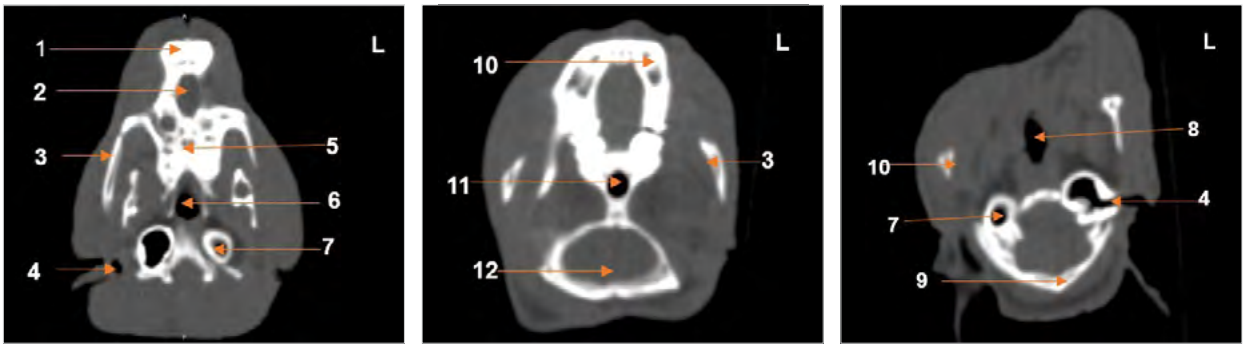

Figure 3 Transverse CT images at the cranial level of a male grasscutter (*Thryonomys swinderianus*)

1. Incisors; 2. Palatine fissure; 3. Zygomatic arch; 4. Tympanic cavity; 5. Palatine bone; 6. Choana; 7. Tympanic bulla; 8. Trachea; 9. Parietal bone; 10. Mandibles; 11. Nasopharynx; 12. Olfactory region

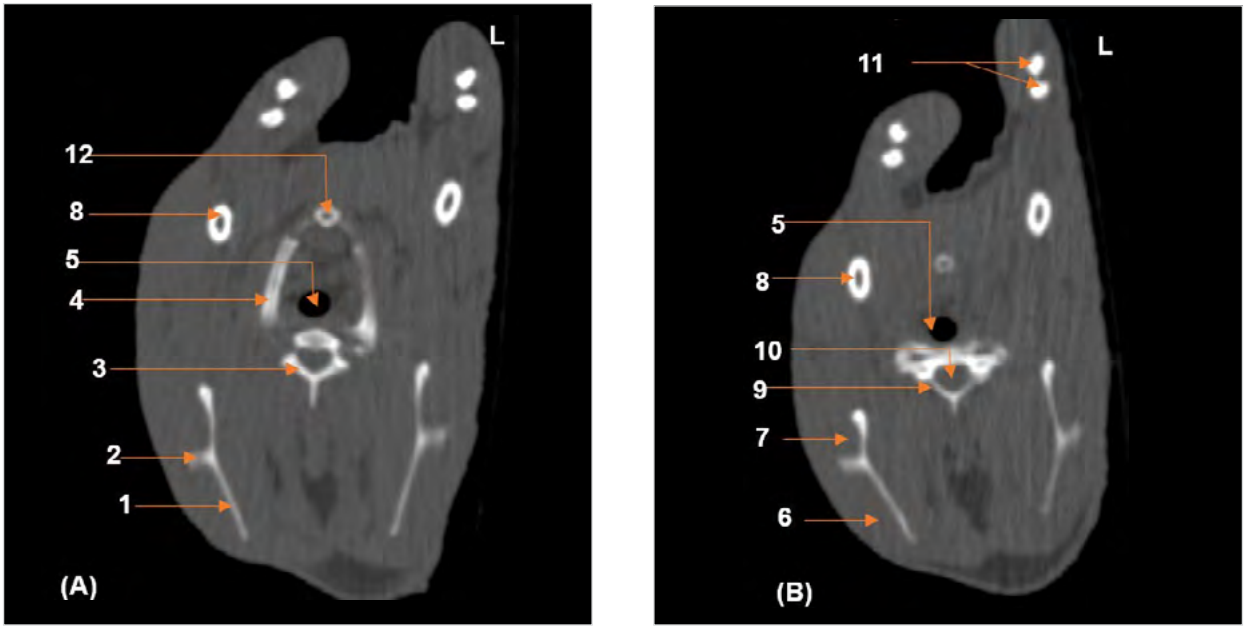

Figure 4 Cross-sectional CT-scans at the level of C7 (A) and T1 (B) vertebrae in the thoracic cavity of male and female grasscutters

1. Scapula; 2. Scapular spine; 3. First thoracic vertebra (T1); 4. First rib; 5. Trachea; 6. Supraspinatus muscle; 7. Infraspinatus muscle; 8. Humerus; 9. Seventh cervical vertebra (C7); 10. Medullary canal; 11. Radius and ulna; 12. Sternum

side, showed the presence of intraluminal gas. The colon was identified through its various segments. Additionally, abdominal and intestinal fat masses were apparent on Figure 9.

In males, the prostate and os penis could not be visualized, whereas in females, the ovaries and uterine horns were not visible. The urinary bladder was clearly delineated on Figure 9 with a homogeneous appearance, and its size varied depending on its content.

As shown on Figure 10, the analysis of CT sections

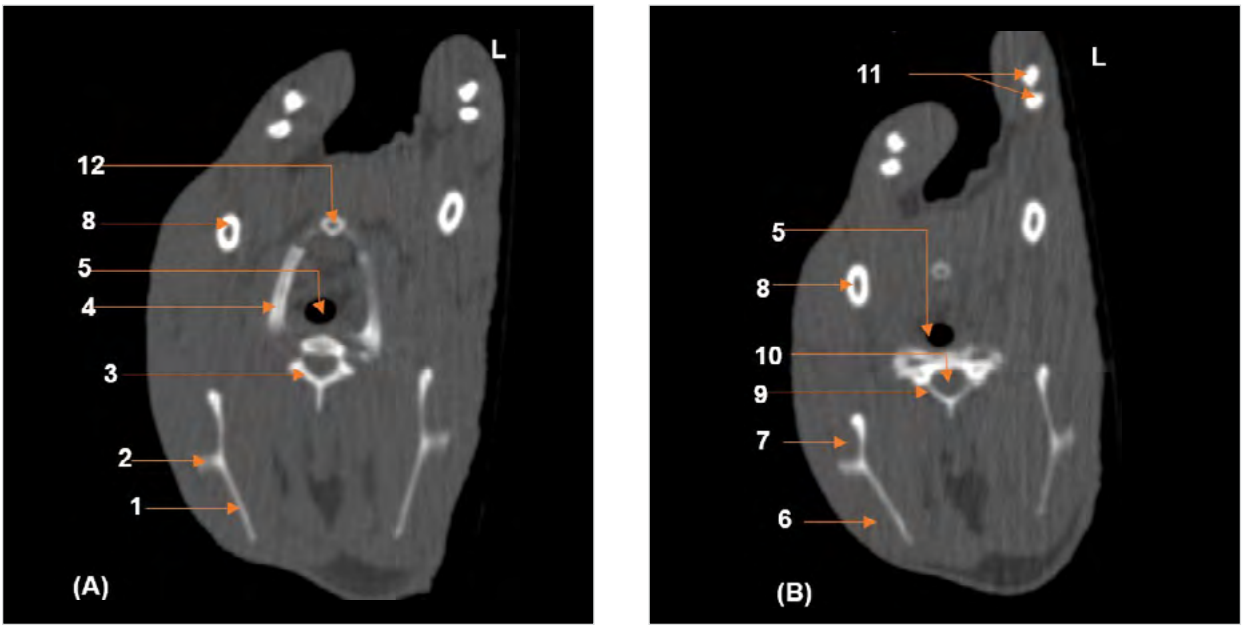

Figure 5 Computed tomography images showing the thoracic cavity using Minimum Intensity Projection (MinIP) (A) and a transverse section at T8 level (B) in a grasscutter

1. Trachea; 2. Right main bronchus; 3. Left main bronchus; 4. Oesophagus; 5. Left lung; 6. Right lung; 7. Heart; 8. Eighth thoracic vertebra (T8); 9. Vena cava; 10. Aorta; 11. Hand

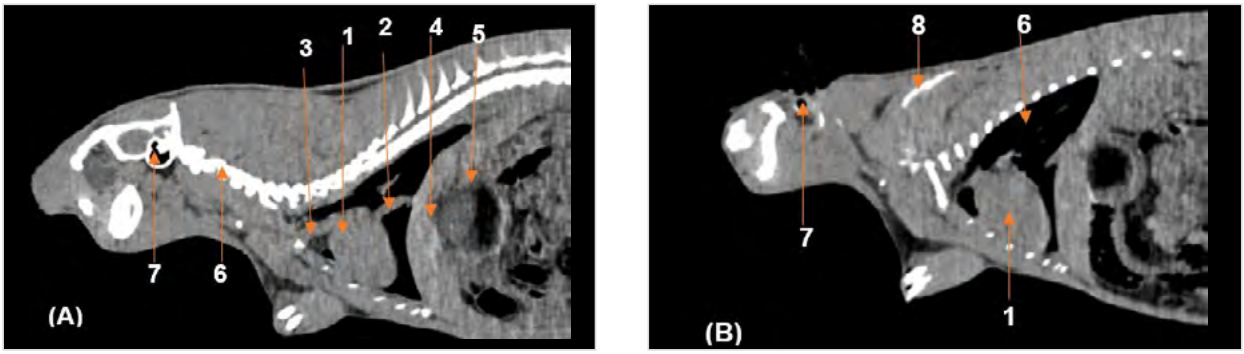

Figure 6 Sagittal CT images of the thoracic cavity in a male grasscutter (A) and a female grasscutter (B)

1. Heart; 2. Caudal vena cava; 3. Cranial vena cava; 4. Liver; 5. Stomach; 6. Left lung; 7. Tympanic bulla; 8. Scapula

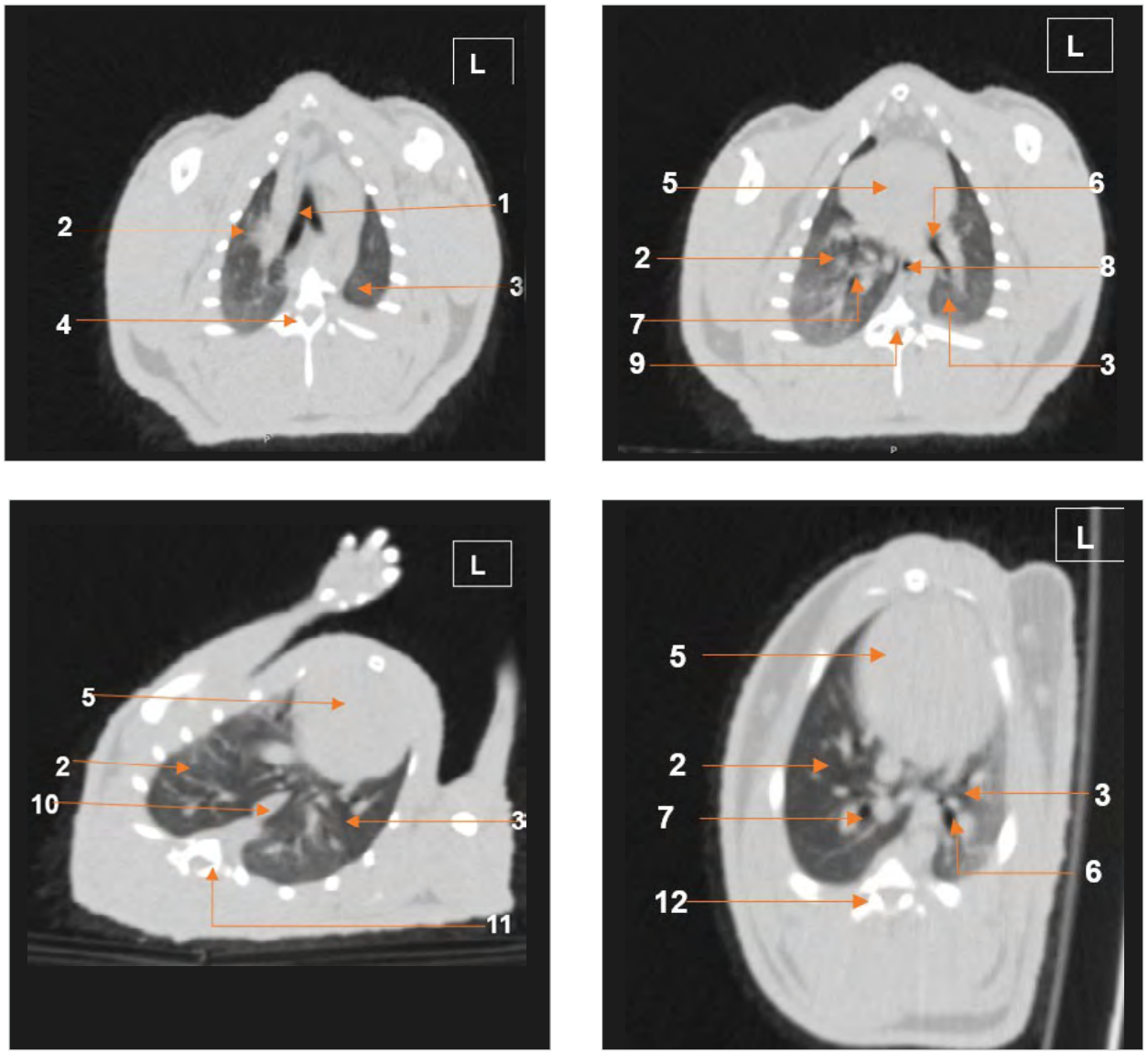

Figure 7 Transverse CT images of the thoracic cavity using a pulmonary window filter

1. Bronchial bifurcation; 2. Right lung; 3. Left lung; 4. Eighth thoracic vertebra (T8); 5. Heart; 6. Left main bronchus; 7. Right main bronchus; 8. Trachea; 9. Ninth thoracic vertebra (T9); 10. Oesophagus; 11. Tenth thoracic vertebra (T10); 12. Seventh thoracic vertebra (T7)

between L2 and L5 revealed both kidneys, with the left kidney showing close anatomical association with the spleen. However, the cortex and medulla could not be differentiated on these images. The ureters were not visualized, although the renal hilum could be identified.

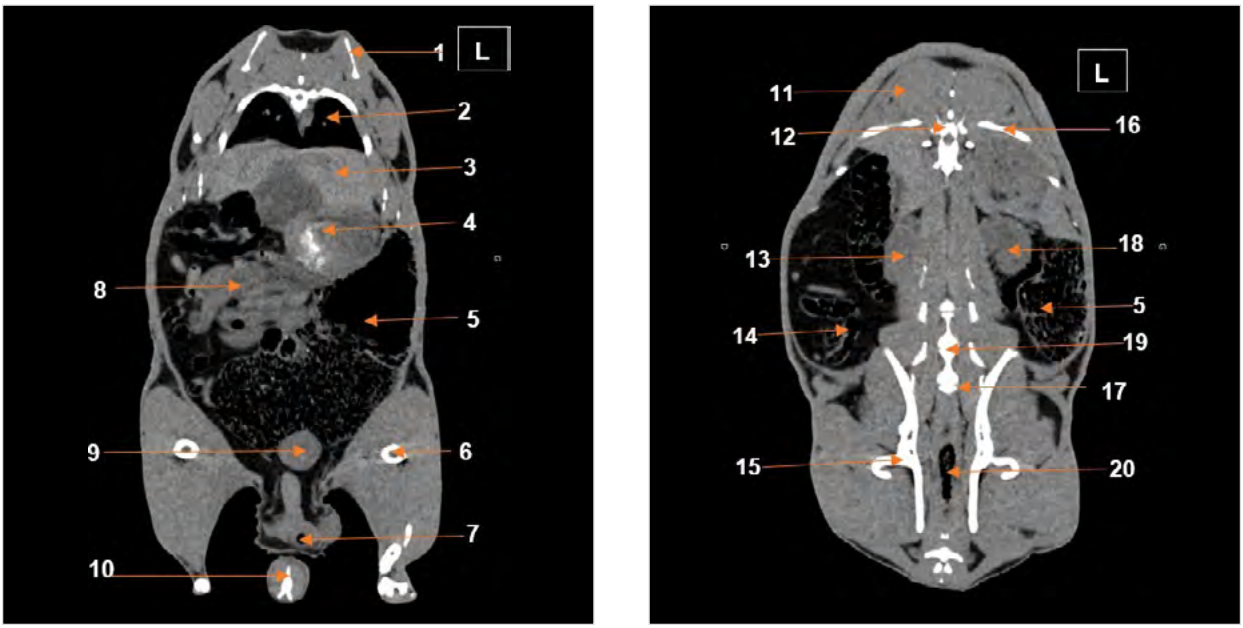

Figure 8 Cross-sectional CT images of the grasscutter's abdomen at the levels of T10 (A) and T13 (B)

1. Liver; 2. Right lung; 3. Heart; 4. Left lung; 5. Tenth thoracic vertebra (T10); 6. Pyloric part of the stomach; 7. Duodenum; 8. Funique part of the stomach; 9. Spleen; 10. Thirteenth thoracic vertebra (T13)

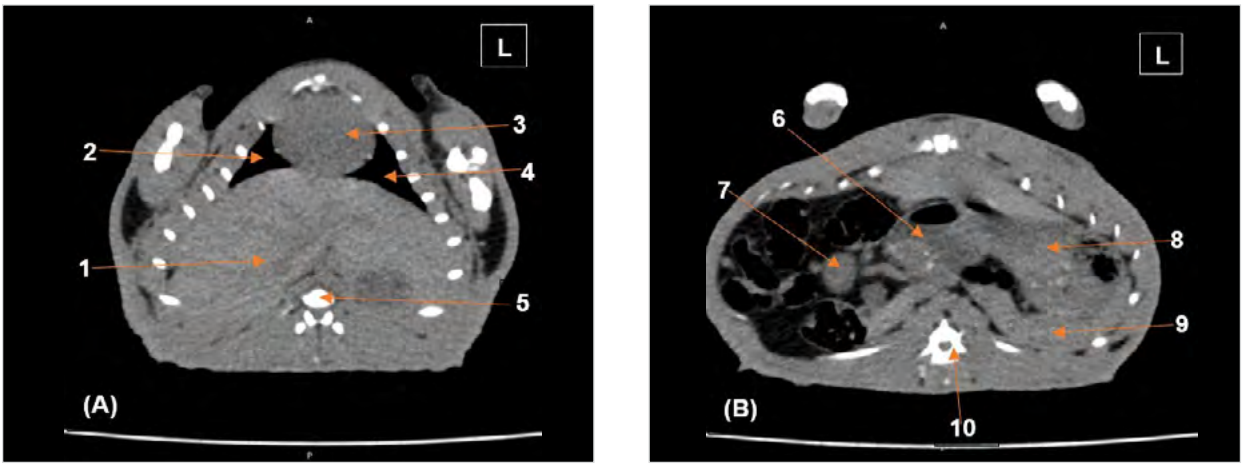

Figure 9 Dorsal and coronal CT-slices of the thoracic and abdominal regions of the grasscutter

1. Scapula; 2. Left lung; 3. Liver; 4. Stomach; 5. Cecum; 6. Femur; 7. Anus; 8. Intestinal mass; 9. Urinary bladder; 10. Coccygeal vertebra; 11. Longissimus thoracis muscle; 12. Twelfth thoracic vertebra (T12); 13. Right kidney; 14. Transverse colon; 15. Coxal bone; 16. Twelfth rib (R12); 17. First sacral vertebra (S1); 18. Left kidney; 19. Sixth lumbar vertebra (L6); 20. Descending colon

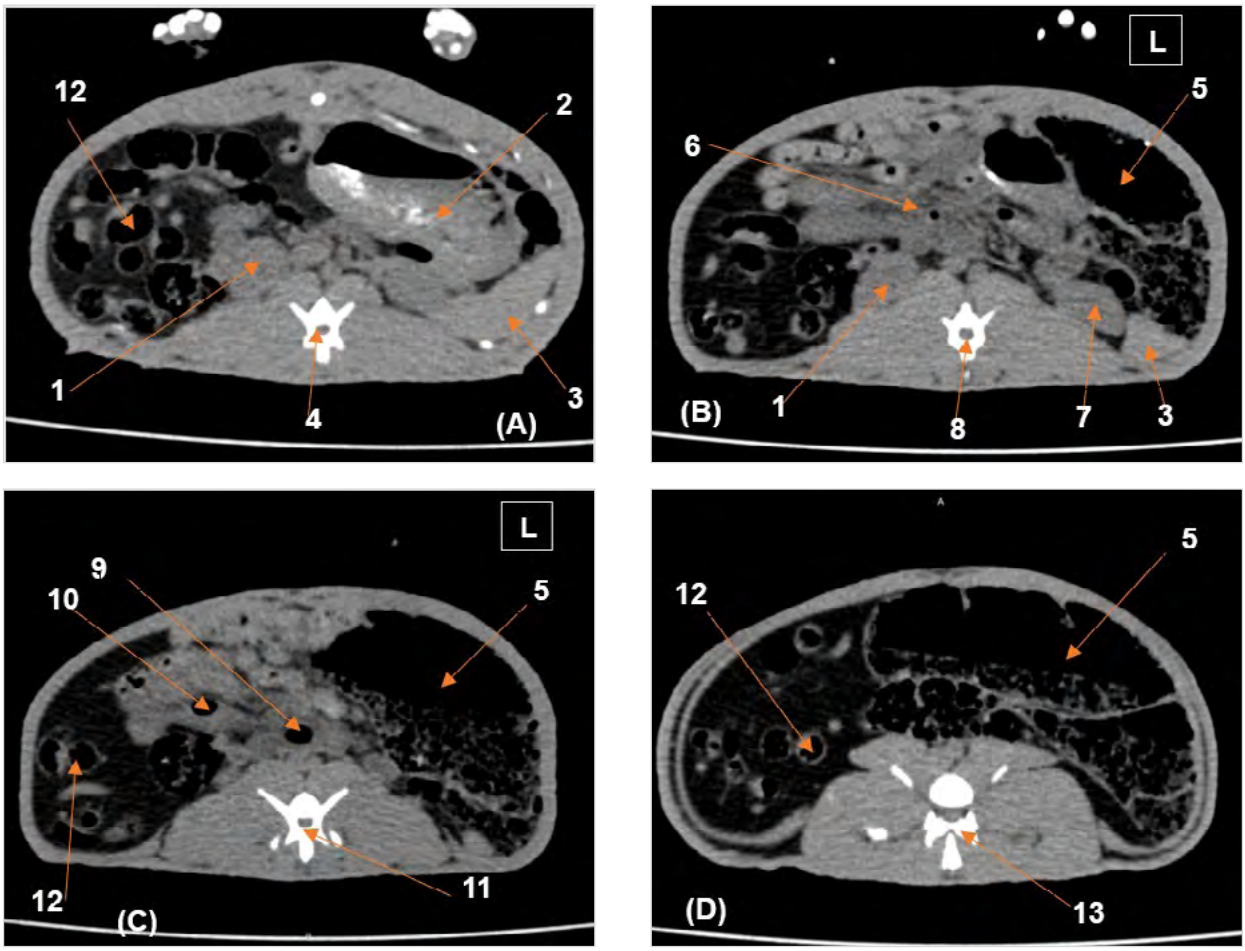

Figure 10 Cross-sectional CT-views of the abdomen at L1, L2, L3, and L5in the grasscutter

1. Right kidney; 2. Stomach; 3. Spleen; 4. First lumbarvertebra (L1); 5. Cecum; 6. Jejunum; 7. Left kidney; 8. Second lumbar vertebra (L2); 9. Descending colon; 10. Ascending colon; 11. Third lumbar vertebra (L3); 12. Transverse colon; 13. Fifth lumbar vertebra (L5)

DISCUSSION AND CONCLUSION

This study, the first to describe the tomodensitometric (CT) features of various internal organs in the greater cane rat or grasscutter (*Thryonomys swinderianus*), focused on comparing the obtained findings with existing data from other mammalian species. On CT images, bones appeared clearly hyperattenuating, and transverse sections of the head and cervical region distinctly depicted the mandibles, tracheal lumen, nasopharynx, and olfactory passages. These results confirm the high spatial resolution of CT imaging for skeletal and dental structures, as previously reported by Boussarie (2014). In clinical practice, CT is commonly employed in this region for detecting rhinitis, vestibular syndromes, and other cranial pathologies (Boussarie, 2014).

The thoracic cavity of the greater cane rat was relatively small, with reduced pulmonary volume, a feature also observed in rabbits (Müllhaupt et al., 2017). The heart occupied a substantial portion of the thoracic cavity, particularly within the cranial and middle mediastinum, as confirmed in this study by CT. These findings mirror those previously described in rabbits using both radiography and CT (Müllhaupt et al., 2017).

Interestingly, the anatomical position of the cardiac apex in the greater cane rat appeared variable across individuals, with a tendency toward a midline orientation rather than the typical left-sided position observed in dogs and cats (Kadja et al., 2007), and

occasionally in aulacodes as well (Hoey et al., 2013). A similar variability has also been reported in rabbits (Müllhaupt et al., 2017). The evaluation of the major mediastinal vessels was limited by the absence of intravenous contrast administration, which would have enabled simultaneous opacification of cardiac chambers and vessels, facilitating detailed analysis. Between T2 and T11, the lungs of the greater cane rat demonstrated similar shape and distribution to those of the rabbit (Müllhaupt et al., 2017). On transverse sections, the diaphragm was often indistinct from the liver, likely due to their anatomical proximity, an appearance also noted in dogs and rabbits. The liver, primarily located between T11 and T13, exhibited a lobar arrangement comparable to that described in rabbits (Daggett et al., 2021). In the abdominal cavity, several digestive organs could be readily identified on CT images, although contrast enhancement would have further improved image quality. The stomach, caecum, and colon were clearly distinguishable, consistent with findings in other small mammals. Similarly, the kidneys and urinary bladder were easily identified on tomodensitometric images, as has been previously reported in dogs, cats, rabbits, ferrets, and lemurs (Calandra, 2016; Huber, 2016; Raharison, 2008). In females, the ovaries and uterine horns could not be visualized clearly, likely due to their attenuation values being similar to those of surrounding musculature. The prostate gland could not be identified in male individuals. This may be attributed to its small size and the limited contrast resolution between the gland and surrounding soft tissues on non-enhanced images (Raharison, 2008). Despite the absence of contrast, CT remains a valuable tool for assessing the condition of thoracic and abdominal organs.

Overall, this study was conducted to investigate the normal tomodensitometric anatomy of clinically healthy greater cane rats. Computed tomography is recognized as being superior to conventional radiography in the evaluation of internal diseases in small mammals (Müllhaupt et al., 2017). Due to their anatomical characteristics and physiological similarities to lagomorphs, greater cane rats, like rabbits (James et al., 2016), may serve as potential animal models for experimental research in biomedical sciences (Müllhaupt et al., 2017). Dorsal recumbency provided satisfactory image quality during scanning. However, mechanical limitations of the restraint device occasionally hindered consistent positioning. Lateral recumbency resulted in suboptimal visualization of left-sided structures. Similar positioning challenges have been reported in rabbits, guinea pigs, and lemurs, for whom sternal or ventral recumbency is preferred to optimize anatomical assessment (Boussarie, 2014; Buch et al., 2022; Calandra, 2016; Hoey et al., 2013; Huber, 2016; Husté, 2016; Mackey et al., 2008; Müllhaupt et al., 2017; Raharison, 2008; Zotti et al., 2009). This study provides preliminary species-specific anatomical information on the greater cane rat obtained through computed tomography. The results demonstrate that CT imaging, even without contrast enhancement, allows identification of major digestive reservoirs, the liver, spleen, certain urinary organs, and bony structures. These data are essential to advance research in health, nutrition, and reproduction of this species and may serve as a reference for future anatomical and tomographic studies.

The prospects offered by this study are promising. The introduction of contrast agents in future CT examinations could enable better visualization of organs and soft tissues, thereby providing a more detailed understanding of the greater cane rat's internal anatomy. Correlating CT images with traditional anatomical sections would also help validate and refine the observations, leading to a more precise and comprehensive anatomical mapping.

Furthermore, the anatomical information obtained could be applied to the diagnosis and treatment of diseases in greater cane rats, facilitating more targeted and effective medical interventions. CT images could also serve as educational tools for training veterinarians and researchers in comparative anatomy and medical imaging. Given that the greater cane rat is consumed in sub-Saharan Africa, this work may prove useful for assisting post-mortem inspection. Finally, an improved understanding of the greater cane rat's anatomy could support conservation and captive breeding programs by optimizing the care and living conditions of these animals. By combining various imaging techniques and anatomical approaches, this research paves the way for a rewarding exploration of the greater cane rat's anatomy, with potential applications across diverse scientific and practical fields.

ACKNOWLEDGEMENTS

The authors thank Islamic Development Bank (IsDB) and the Government of Togo for funding this project. We also extend our sincere appreciation to the private hospital Saint Sauveur of Kara for granting access

to its CT imaging facility, which was instrumental in conducting this study.

CONFLICT OF INTEREST

The authors declared that there is no conflict of interest.

CONTRIBUTIONS

Concept – AA, CG, MT; Design – AA, CG, MT; Supervision – CG, MT; Funding – AA; Materials – AA; Data Collection and Processing – AA; Analysis and Interpretation – AA; Literature Search – AA; Writing Manuscript – AA; Critical Review – CG, MT.

REFERENCES

Ajayi IE, Ojo SA, Ayo JO, Ibe CS. 2010. Histomorphometric studies of the urinary tubules of the African grasscutter (*Thryonomys swinderianus*). J Vet Anat, 3(1), 17–23.

Ananivi S, Hounakey MA, Laleye CM, Edem JY, Broalet MYE, Amégnona A, et al. 2025. Anatomical study of the coronary arteries of the grasscutter (*Thryonomys swinderianus,* Temminck 1827). 2025. Original Res Artic, (1), 9109–22. doi:10.16965/ijar.2024.243.

Boussarie D. 2014. La tomodensitométrie chez le lapin de compagnie: réalisation pratique et indications. Bull Acad Vét Fr, 167(1), 11–15. doi:10.4267/2042/53716.

Broalet E, Tako A, Zunon-Kipre Y, Ouattara D, Kouakou F. 2012. Sur l'anatomie de l'aulacode (*Thryonomys swinderianus,* Temminck, 1827): revue de littérature. In: Morphologie, vol. 96, p. 100. Elsevier BV.

Buch D, Saldanha A, de Almeida Santos I, Muehlbauer E, Ueno Gil EM, Froes TR, et al. 2022. Computed tomographic findings of the gastrointestinal tract in rabbits. J Exotic Pet Med, 42, 11–19. doi:10.1053/j.jepm.2022.03.005.

Calandra M. 2016. Mise au point d'un atlas en ligne d'images tomodensitométriques normales du furet (*Mustela putorius furo*). Thèse d'exercice, École nationale vétérinaire de Toulouse-ENVT, Toulouse, p72.

Daggett A, Loeber S, Le Roux AB, Beaufrere H, Doss G. 2021. Computed tomography with Hounsfield unit assessment is useful in the diagnosis of liver lobe torsion in pet rabbits (*Oryctolagus cuniculus*). Vet Radiol Ultrasound, 62(2), 210–17. doi:10.1111/vru.12939.

Hoey S, Drees R, Hetzel S. 2013. Evaluation of the gastrointestinal tract in dogs using computed tomography. Vet Radiol Ultrasound, 54(1), 25–30. doi:10.1111/j.1740-8261.2012.01969.x.

Huber AP. 2016. Mise au point d'un atlas en ligne d'images tomodensitométriques normales du lapin. Thèse d'exercice, École nationale vétérinaire de Toulouse-ENVT, Toulouse, p30.

Husté D. 2016. Mise au point d'un atlas en ligne d'images tomodensitométriques normales du cobaye (Cavia porcellus). Thèse d'exercice, École nationale vétérinaire de Toulouse-ENVT, Toulouse, p65.

Ibe CS, Ogbonnaya O, Ikpegbu E, Ani NV. 2023. Anatomical studies on the African grasscutter (*Thryonomys swinderianus*), a key component of the minilivestock industry in Nigeria. Anat Rec, 306(1), 226–34. doi:10.1002/ar.25049.

Ibe CS, Ukaha RO, Njoku NU, Jeremiah KT, Ukweze CO, Tchokote EY, et al. 2024. Radiologic indices of cardiac mensuration in the African grasscutter (*Thryonomys swinderianus*). Veterinaria, 73(1), 13–24. doi:10.51607/2233 1360.2024.73.1.13.

James EY, Broalet E, Darre T, Zunon-Kipre Y, Agbonon A, Amouzouvi G, et al. 2016. Etude anatomique du système artériel carotidien de l'aulacode (*Thryonomysswinderianus*, Temminck 1827). EurSci J, 12(12), 246. doi:10.19044/esj.2016.v12n12p246.

Kadja M, Mensah GA, Akomedi TC, Pomalegni SCB. 2007. Topographie des viscèresthoraciques et abdominaux de l'aulacode (*Thryonomys swinderianus*) : projections pariétales droites et gauches. Bull Rech Agron Bénin, 55, 36–44.

Mackey EB, Hernandez-Divers SJ, Holland M, Frank P. 2008. Clinical technique: application of computed tomography in zoological medicine. J Exotic Pet Med, 17(3), 198–209. doi:10.1053/j.jepm.2008.05.007.

Mensah AG, Mensah ERCKD, Pomalegni BC. 2007. Guide pratique de l'aulacodiculture. Cotonou: Bibliothèque Nationale du Bénin.

Mpagike FH, Makungu M. 2023. Osteology and radiographic anatomy of the thoracic limb of the greater cane rat (*Thryonomys swinderianus*). Anat Histol Embryol, 52(3). doi:10.1111/ahe.12898.

Müllhaupt D, Wenger S, Kircher P, Pfammatter N, Hatt JM, Ohlerth S. 2017. Computed tomography of the thorax in rabbits: a prospective study in ten clinically healthy New Zealand White rabbits. Acta Vet Scand, 59(1), 72. doi:10.1186/s13028-017-0340-x.

Mustapha OA, Ajadi TA, Mustapha OO, Olaolorun FA, Popoola ES, Olude MA, et al. 2019. Sonographic features of gestation in the developing greater cane rat (*Thryonomys swinderianus*). Bull Anim Health Prod Afr, 67, 247–54.

Raharison FSV. 2008. Etude anatomique d'une espèce de lémurien (*Eulemur fulvus*) : coupes topographiques et

tomodensitométriques du thorax, de l'abdomen et du bassin. Application à la pratique de l'échographie du cœur et des reins. Thèse, École nationalevétérinaire de Toulouse-ENVT, Toulouse.

Tarbell AL, Fischetti AJ. 2020. Diagnostic imaging. In: Quesenberry KE, Orcutt CJ, Mans C, Carpenter JW (Eds), Ferrets, Rabbits, and Rodents Clinical Medicine and Surgery, 3rd ed., pp. 559–68. Philadelphia, PA: W.B. Saunders. doi:10.1016/B978-0-323-48435-0.00038-1.

Winn FA. 2006. Atlas radiographique du lapin de compagnie. Thèse d'exercice, École nationale vétérinaire de Toulouse-ENVT, Toulouse, p122

Yapi YM. 2013. Physiologie digestive de l'aulacode (*Thryonomys swinderianus*) en croissance. Thèse, Institut National Polytechnique de Toulouse, Toulouse.

Zotti A, Banzato T, Cozzi B. 2009. Cross-sectional anatomy of the rabbit neck and trunk: comparison of computed tomography and cadaver anatomy. Res Vet Sci, 87(2), 171–6. doi:10.1016/j.rvsc.2009.02.003.

Kompjuterizovana tomografska (CT) studija anatomije divivskog trstičnog štakora (*Thryonomys swinderianus,* Temminck 1827): Preliminarna opažanja

SAŽETAK

Divovski trstični štakor (*Thryonomys swinderianus*) je afrički glodar čiji se uzgoj djelimično razvio zbog sve većeg naučnog interesa. Ovaj rad ima za cilj istražiti unutrašnju anatomiju divovskog afričkog štakora (*Thryonomys swinderianus*) pomoću kompjuterizovane tomografije (CT). Šest jedinki divovskog štakora, prosječne starosti 345±45.63 dana, različitog spola i težine, podvrgnuto je opštoj anesteziji pomoću mješavine ketamina i ksilazina, nakon čega je izvršeno CT skeniranje. Dobijeni su volumetrijski snimci koji su rekonstruisani korištenjem specifičnih filtera: „torakalno ili plućno tkivo", „abdominalno tkivo" i „koštano tkivo".

Unutar torakalne šupljine identifikovane su strukture kao što su dušnik, bronhiji, pluća, jednjak, srce i aorta. U abdominalnoj šupljini uočena je jetra koja se prostire poprečno s lijeva na desno. Želudac, koji je sadržavao mineralni materijal, kao i slezena, bili su jasno vidljivi. Također su bili uočljivi bubrezi, pri čemu se lijevi bubreg nalazio nešto kranijalnije od desnog. Mokraćna bešika je bila prepoznatljiva, zavisno od stepena njenog punjenja. Isti ovi organi prethodno su opisani kod kunića, lemura i zamoraca pomoću CT snimanja, što podržava komparativne anatomske analize. Međutim, ureteri nisu mogli biti vizualizirani na trenutnim snimcima.

Ovoistraživanje predstavlja prvo anatomsko ispitivanje divovskog afričkog štakora zasnovano na CT snimanju i pruža vrijedne uvide za primijenjena istraživanja o zdravlju ove vrste.

Ključne riječi: Anatomija, kompjuterizovana tomografija, divovski trstični štakor, rentgenski snimak